Molecular Biology of the Cell
Vol. 21, 95–105, January 1, 2010

Phosphatidylinositol 3,4,5-trisphosphate Localization in Recycling Endosomes Is Necessary for AP-1B–dependent Sorting in Polarized Epithelial Cells

Ian C. Fields, Shelby M. King, Elina Shteyn, Richard S. Kang, and Heike Fölsch

Department of Biochemistry, Molecular Biology and Cell Biology, Northwestern University, Evanston, IL 60208

Submitted January 13, 2009; Revised October 5, 2009; Accepted October 20, 2009
Monitoring Editor: Sandra Lemmon

Polarized epithelial cells coexpress two almost identical AP-1 clathrin adaptor complexes: the ubiquitously expressed AP-1A and the epithelial cell–specific AP-1B. The only difference between the two complexes is the incorporation of the respective medium subunits μ1A or μ1B, which are responsible for the different functions of AP-1A and AP-1B in TGN to endosome or endosome to basolateral membrane targeting, respectively. Here we demonstrate that the C-terminus of μ1B is important for AP-1B recruitment onto recycling endosomes. We define a patch of three amino acid residues in μ1B that are necessary for recruitment of AP-1B onto recycling endosomes containing phosphatidylinositol 3,4,5-trisphosphate [PI(3,4,5)P_3]. We found this lipid enriched in recycling endosomes of epithelial cells only when AP-1B is expressed. Interfering with PI(3,4,5)P_3 formation leads to displacement of AP-1B from recycling endosomes and missorting of AP-1B–dependent cargo to the apical plasma membrane. In conclusion, PI(3,4,5)P_3 formation in recycling endosomes is essential for AP-1B function.

INTRODUCTION

During embryonic development, epithelial cells polarize their plasma membrane into distinct apical and basolateral domains separated by tight junctions, which prevent mixing of lipid and protein content between the two domains. Once established, this polarity has to be maintained for proper tissue functions, meaning that internalized and newly synthesized transmembrane proteins destined for the apical or basolateral plasma membrane have to be correctly sorted in the endocytic and/or secretory system (Mostov *et al.*, 2003; Rodriguez-Boulan *et al.*, 2005; Fölsch, 2008).

Whereas apical sorting information is often encoded in a protein's ectodomain, basolateral sorting signals are frequently composed of peptide signals encoded in the protein's cytoplasmic tail. Among the best-characterized basolateral sorting signals are the tyrosine-based sorting signals, which are related to endocytic and lysosomal sorting signals. Tyrosine-based signals are known to interact with the medium subunits of heterotetrameric clathrin adaptor (AP) complexes (Nakatsu and Ohno, 2003). There are four distinct classes of AP complexes (AP-1 to AP-4), each consisting of two large subunits (γ, α, δ, ε, and β1–β4), one medium subunit (μ1–μ4), and a small subunit (σ1–σ4; Brodsky *et al.*, 2001). AP-1, AP-3, and AP-4 each localize to the *trans*-Golgi network (TGN) or endosomes, whereas AP-2 is localized at the plasma membrane to facilitate clathrin-mediated endocytosis (Nakatsu and Ohno, 2003).

Most polarized epithelial cells coexpress the epithelial cell–specific AP-1B complex in addition to the ubiquitously expressed AP-1 (now named AP-1A). Both complexes differ only in the incorporation of their respective medium subunits μ1A or μ1B, which are 79% identical on the amino acid level (Ohno *et al.*, 1999). Despite this close homology, AP-1A and AP-1B have distinct functions in endosomal/lysosomal sorting or basolateral membrane targeting, respectively. For example, AP-1A cannot substitute for AP-1B in basolateral sorting of transferrin receptors (TfnR) or truncated low-density lipoprotein receptors (LDLR-CT27) that contain only the proximal basolateral sorting determinant (Fölsch *et al.*, 1999; Fields *et al.*, 2007). Likewise, AP-1B cannot facilitate retrieval of the proprotein convertase furin from early endosomes to the TGN when AP-1A is missing (Fölsch *et al.*, 2001). Furthermore, AP-1B, but not AP-1A, has been shown to facilitate the recruitment of the exocyst subunits Exo70 and Sec8 onto AP-1B–positive membranes (Fölsch *et al.*, 2003). The exocyst complex is thought to tether AP-1B vesicles to the basolateral plasma membrane to allow for membrane fusion (Fölsch, 2005). These different functions may in part be explained by the differential localization of AP-1A and AP-1B to the TGN and perinuclear common recycling endosomes, respectively (Gan *et al.*, 2002; Fölsch *et al.*, 2003).

The recruitment of adaptor complexes to different membranes may be the result of interactions with the small GTPase ADP-ribosylation factor 1 (Arf1) and preferences for specific membrane lipids. The TGN-localized AP-1A, AP-3,

This article was published online ahead of print in *MBC in Press* (http://www.molbiolcell.org/cgi/doi/10.1091/mbc.E09–01–0036) on October 28, 2009.

Address correspondence to: Heike Fölsch (h-folsch@northwestern.edu).

Abbreviations used: Arf, ADP-ribosylation factor; CI-MPR, cation-independent mannose 6-phosphate receptor; Grp1, general receptor for phosphoinositides-1; LDLR, low-density lipoprotein receptor; mRFP, monomeric red fluorescent protein; PI(3)P, phosphatidylinositol 3-phosphate; PI(4)P, phosphatidylinositol 4-phosphate; PI(4,5)P_2, phosphatidylinositol 4,5-bisphosphate; PI(3,4,5)P_3, phosphatidylinositol 3,4,5-trisphosphate; PH, pleckstrin homology; PTB, phophotyrosine binding; PTEN, phosphatase and tensin homolog; TfnR, transferrin receptor.

and AP-4 have all been shown to depend on activated GTP-bound Arf1 for membrane recruitment (Hirst and Robinson, 1998; Robinson and Bonifacino, 2001). In addition, it has been shown that membrane recruitment of AP-1A depends on the lipid molecule phosphatidylinositol 4-phosphate [PI(4)P; Wang *et al.*, 2003]. PI(4)P is enriched at the TGN and it is suspected that PI(4)P binds to both the γ and the μ1A-subunit of AP-1A (Heldwein *et al.*, 2004). The situation is slightly different for AP-2. Here, even though Arf6 has been shown to recruit AP-2 onto liposomes devoid of phosphoinositides in vitro (Paleotti *et al.*, 2005), it is believed that binding of the α- and μ2-subunit to phosphatidylinositol 4,5-bisphosphate [PI(4,5)P_2] is sufficient for specific membrane recruitment of AP-2 in vivo (Collins *et al.*, 2002). Interestingly, recent findings suggest that AP-2 itself targets a specific PI(4)P 5-kinase onto the plasma membrane that is needed to generate PI(4,5)P_2 at the site of endocytosis (Bairstow *et al.*, 2006; Krauss *et al.*, 2006). In contrast, it is not known how AP-1B is recruited onto recycling endosomes. Moreover, a signature lipid for recycling endosomes has not been defined (Roth, 2004).

In this study we define a signature lipid for common recycling endosomes in polarized epithelial cells. We show that phosphatidylinositol 3,4,5-trisphosphate [PI(3,4,5)P_3] accumulation in recycling endosomes is dependent on AP-1B expression. Importantly, PI(3,4,5)P_3 is needed for localization of AP-1B in recycling endosomes and basolateral sorting of AP-1B–dependent cargos. Furthermore, mutagenesis of only three amino acid residues in the C-terminus of μ1B completely abolishes AP-1B's recruitment onto recycling endosomes. These data explain at least partially the different sorting functions and different intracellular localizations of AP-1A and AP-1B.

MATERIALS AND METHODS

Constructs and Generation of Fusion Proteins

To generate $\mu1B^{loca}$-HA, site-directed mutagenesis was performed (QuikChange; Stratagene, La Jolla, CA) using full-length μ1B with an internal hemagglutinin (HA)-tag, μ1B-HA, in pCB6 (Fölsch *et al.*, 2001) as template. μ1B-HA was mutated with corresponding sense and anti-sense primers. The sense primer was 5′-GGCAGCGCCAAGTATGTGCCGGAGAACAGCGAGGTGATTTGGAGTATTAAGTCTTTC-3′. Subsequently, LLC-PK1 cells were transfected with μ1B-HA constructs using LipofectAMINE (Invitrogen, Carlsbad, CA) as described below. Positive transfectants were selected and maintained as described previously (Fölsch *et al.*, 2001).

For generating T7-PTEN (phosphatase and tensin homolog) in pRKV, we obtained the *human PTEN* gene from Thermo Fisher Scientific (clone ID 3937787; Huntsville, AL) and used it as a PCR template together with the following N- and C-terminal primers: 5′-GCGCGGATCCATGGCTAGCATGACTGGTGGACAGCAAATGGGTATGACAGCCATCATCAAAGAGATCGTTAGC-3′ and 5′-GCGCAAGCTTTCAGACTTTTGTAATTTGTGTATGCTG-3′, respectively. PCR products were cloned as BamHI/HindIII fragments into pRKV.

To clone red fluorescent protein (RFP)-PH–general receptor for phosphoinositides-1 (Grp1), we purchased the *human Grp1* gene from Thermo Fisher Scientific (clone ID 2984886) and amplified PH-Grp1 (amino acids 264-381) using the following N- and C-terminal primers: 5′-GCGCAGATCTATGAACCCCGACCGCGAGGGCTGGCTC-3′ and 5′-GCGCAAGCTTTCATCTGCTGATACTGGCTTTGATG-3′, respectively. PCR products were cloned as BglII/HindIII fragments into RFP-containing pRKV in frame directly behind monomeric RFP (mRFP; Fields *et al.*, 2007).

To generate PTB-ARH (phophotyrosine binding–autosomal recessive hypercholesterolemia) tagged with mRFP, we first amplified RFP using cellubrevin-RFP as template (Fields *et al.*, 2007), and the following N- and C-terminal primers: 5′-GCGCGGATTCATGGCCTCCTCCGAGGACGTCATC-3′and 5′-GCGCAAGCTTTTAGGCGCCGGTGGAGTGGCGGCCCTC-3′, respectively. RFP was cloned as a BamHI/HindIII fragment into pRKV. We then amplified PTB-ARH (amino acids 1-179) using *human ARH* (Thermo Fisher Scientific; clone ID 5197824) as template and the following N- and C-terminal primers: 5′-CGCGGAATTCATGGACGCGCTCAAGTCGGCGGGG-3′ and 5′- CGCGGGATCCTTTCTCTTCCTTGGACACCTGCCAAAACTCAAAGG-3′, respectively. PTB-ARH PCR products were cloned as EcoRI/BamHI fragments in frame in front of RFP into pRKV.

To clone RFP-tagged tandem FYVE, we first cloned mRFP as EcoRI/BamHI fragments into pRKV (Fields *et al.*, 2007). Subsequently, the FYVE domain (amino acids 1325-1411) of early endosome antigen 1 (EEA1) was amplified using *mouse EEA1* (Thermo Fisher Scientific; clone ID 30545051) as template and the following respective N- and C-terminal primers: 5′-GCGCGGATCCATGGCGGCCGTGCAGGAGCTGGGC-3′ and 5′-GCGCAAGCTTTCTAGAACTTCCTCCTTGCAAATCATTGAAGC-3′. The C-terminal primer introduces a linker (SG) and two restriction sites (XbaI and HindIII). PCR products were cloned as BamHI/HindIII fragments in frame behind mRFP into pRKV. Finally, we amplified the FYVE domain a second time. This time the N- and C-terminal primers were as follows: 5′-GCGCTCTAGAGCGGCCGTGCAGGAGCTGGGC-3′ and 5′-GCGCAAGCTTTTATCCTTGCAAATCATTGAAGC-3′, respectively. The resulting PCR products were cloned as XbaI/HindIII fragments in frame behind the first FYVE domain resulting in RFP-FYVE-XbaI(=RS)-SG-FYVE in pRKV.

Plasmids encoding LDLR(Y18A), LDLR-CT27, human TfnR, TGN38, VSVG-ts045-green fluorescent protein (GFP), or RFP-cellubrevin-VW were described previously (Fölsch *et al.*, 2001, 2003; Fields *et al.*, 2007; Nokes *et al.*, 2008). Plasmids encoding PH-Akt-GFP were a gift from Dr. Peter Devreotes (Johns Hopkins School of Medicine, Baltimore, MD), and plasmids encoding GFP-PIPKIγ-90 were a gift from Dr. Pietro De Camilli (Yale University, New Haven, CT).

All constructs were verified by sequencing. No errors were found.

Recombinant Adenoviruses, Antibodies, and Reagents

Defective adenoviruses encoding LDLR-CT27 and LDLR(Y18A) were described previously (Fölsch *et al.*, 1999, 2003; Fields *et al.*, 2007).

Production of recombinant retrovirus encoding shRNA for μ1B knockdown and empty vector control as well as infection and generation of MDCK cells stably expressing these constructs were performed exactly as described previously (Anderson *et al.*, 2005). The plasmids needed for retrovirus production were a gift from Drs. Sandra Maday (University of Pennsylvania, Philadelphia, PA) and Ira Mellman (Genentech, South San Francisco, CA).

Purchased mouse monoclonal antibodies were as follows: anti-HA (16B12) from BabCo (Richmond, CA), anti-T7 antibodies (69522-3) from Novagen (Madison, WI), anti-γ-adaptin (100/3), and anti-β1/β2-adaptin (100/1) were from Sigma (St. Louis, MO). Hybridoma cell lines producing anti-hTfnR (H68.4) or anti-LDLR (C7) were described previously (Fields *et al.*, 2007). Polyclonal antibodies against μ1A/B were from Dr. Linton Traub (University of Pittsburgh, Pittsburgh, PA), polyclonal antibodies against TGN38 were from Dr. Graham Warren (Max F. Perutz Laboratories, Vienna, Austria), polyclonal antibodies against bovine CI-MPR were from Dr. Suzanne Pfeffer (Stanford University, Stanford, CA), and polyclonal antibodies against μ1B were described previously (Fölsch *et al.*, 1999). Secondary antibodies labeled with Alexa fluorophores were purchased from Molecular Probes (Eugene, OR), and HRP- or Cy5-conjugated secondary antibodies were from Jackson ImmunoResearch Laboratories (West Grove, PA). Alexa 488–labeled human Tfn was purchased from Molecular Probes. PI 3-kinase inhibitor LY294002 was purchased from EMD Biosciences (San Diego, CA).

Cell Culture

Madin-Darby canine kidney (MDCK) cells were maintained in MEM containing 7% (vol/vol) fetal bovine serum (FBS), 2 mM L-glutamine, and 100 μg/ml penicillin/streptomycin. LLC-PK1 cells stably transfected with μ1 constructs were grown in α-MEM containing 7% (vol/vol) FBS, 2 mM L-glutamine, 100 μg/ml penicillin/streptomycin, and 1.0 mg/ml Geneticin (Gibco BRL Life Technologies, Rockville, MD). HeLa cells and HEK293 cells were maintained in DMEM containing 10% (vol/vol) FBS, 2 mM L-glutamine, and 100 μg/ml penicillin/streptomycin. All cell lines were grown in a 5% CO_2 incubator at 37°C.

For immunofluorescence analysis, cells were seeded on Alcian blue–coated coverslips or onto coverslips coated with fibronectin/collagen. The fibronectin coating solution contained LHC basal medium with 10 mg/100 ml bovine serum albumin, 3 mg/100 ml bovine collagen I, and 1 mg/100 ml fibronectin. Cells on coverslips were cultured for 2–4 d. To allow for polarization, cells were seeded onto polycarbonate membrane filters at a density of 4×10^5 cells per 12-mm filter (0.4-μm pore size; Transwell units; Corning-Costar, Cambridge, MA) and cultured for 4–6 d with changes of medium in the basolateral chamber every day. In general, cells were fixed in 3% (wt/vol) paraformaldehyde (PFA) for 15 min at RT. After fixation, cells were processed for immunofluorescence essentially as described previously (Fölsch *et al.*, 2003).

For infection of filter-grown MDCK cells with defective adenoviruses, cells were washed once in serum-free, calcium/magnesium-free medium (SMEM$^-$), and 50–100 plaque-forming units/cell of the viruses were added to the apical chamber. After 2-h incubation at 37°C, the medium was exchanged with normal growth medium. The cells were prepared for immunofluorescence analysis 2 d after infection.

Transient transfections were carried out using LipofectAMINE (Invitrogen) according to the manufacturer's protocol, followed by incubation overnight at 37°C. For Tfn uptake assays, cells were transiently transfected with cDNA encoding human TfnR. Twenty-four hours after transfection, cells were starved in serum-free medium for 30 min at 37°C. Cells were then incubated with Alexa-labeled human Tfn (1:100) in serum-free medium for 25 min,

followed by incubation with unlabeled human Tfn (10 mg/ml) for exactly 2 min at 37°C. Cells were washed in ice-cold PBS^{2+} (PBS [0.2 g/l KCl, 0.2 g/l KH_2PO_4, 8 g/l NaCl, and 2.17 g/l $Na_2HPO_4 \times 7\ H_2O$] plus 0.1 g/l $CaCl_2$ and 0.1 g/l $MgCl_2 \times 6\ H_2O$) and fixed and processed for immunofluorescence analysis as described above.

For cell surface staining, the cultures were washed once with ice-cold PBS^{2+} and incubated with antibodies applied to apical and basolateral sides for 15 min to 1 h on ice. Cultures were washed three times with ice cold PBS^{2+} and fixed. Filters were then cut out and stained for immunofluorescence microscopy essentially as described above.

All immunofluorescence preparations were analyzed using a Zeiss confocal microscope (Microsystem LSM 510; Thornwood, NY) with an Axiovert 100 microscope and a Plan-Apochromat 63× objective. Images were adjusted using Adobe Photoshop (San Jose, CA) and combined using Adobe Illustrator.

Statistical Analysis

Statistical analysis of numerical data in Figures 5C and 6 was done by first calculating the mean value and SD from the mean for each experimental condition. The mean value, SD, and n value were then used in a Student's unpaired *t* test (GraphPad, San Diego, CA; QuickCalcs) to determine statistical significance.

Colocalization of PH-Akt-GFP and TfnR in recycling endosomes (see Figures 2C and 3B) or GFP-PIPKIγ-90 and TfnR (see Figure 4B) was analyzed with Volocity 4.4 software. Confocal raw data were imported into Volocity (Improvision, Lexington, MA), and the background threshold of the images was adjusted to the same degree in all images analyzed. We then circled the region of perinuclear TfnR staining as the region of interest for calculation of the overlap coefficient according to Manders (Manders *et al.*, 1993). The data are expressed as % overlap. Statistical analysis was then performed as described in the previous paragraph.

RESULTS

Recycling Endosomes Contain PI(3,4,5)P_3

To gain a better understanding of the lipid composition in recycling endosomes, we transiently expressed different lipid-sensing domains in MDCK cells and analyzed their localization with respect to TfnR, a marker for perinuclear common recycling endosomes or peripheral early endosomes. As lipid sensors we chose the FYVE domain of EEA1 as a probe for phosphatidylinositol 3-phosphate [PI(3)P], the PTB domain of ARH as a probe for PI(4,5)P_2, and the pleckstrin homology (PH) domain of Akt as a probe for PI(3,4,5)P_3 (Di Paolo and De Camilli, 2006). Both PI(4,5)P_2 and PI(3,4,5)P_3 were shown previously to play a role in organizing polarized epithelial cysts (Martin-Belmonte *et al.*, 2007).

To test for the distribution of PI(3)P in MDCK cells, we cotransfected coverslip grown cells with cDNA encoding a tandem FYVE domain chimera tagged with mRFP. Tandem FYVE domain constructs are used to increase the binding affinity of this domain to PI(3)P (Gillooly *et al.*, 2000). Six hours after transfection, cells were stained for endogenous TfnR. As expected, we found the FYVE domain localizing to peripheral endosomal structures (Figure 1A). We confirmed by Tfn uptake for 7 min that these structures are early endosomes (not shown). Importantly, we did not observe colocalization between the FYVE domain and TfnR in perinuclear recycling endosomes (Figure 1A). Next we expressed mRFP-tagged PTB-ARH in MDCK cells grown on coverslips. We found PTB-ARH-RFP primarily localizing to the plasma membrane (Figure 1B). Finally, we transiently expressed the PH domain of Akt fused to GFP (PH-Akt-GFP) in coverslip-grown MDCK cells. The PH domain of Akt is known to bind relatively specifically to PI(3,4,5)P_3 in vitro with a threefold less binding affinity to PI(3,4)P_2 (James *et al.*, 1996) and is commonly used to monitor PI(3,4,5)P_3 localization in vivo (Di Paolo and De Camilli, 2006). We found PH-Akt-GFP localizing to the plasma membrane as well as to TfnR-positive recycling endosomes (Figure 1C).

Taken together, we found colocalization of PH-Akt-GFP with TfnR in recycling endosomes. In contrast, we observed

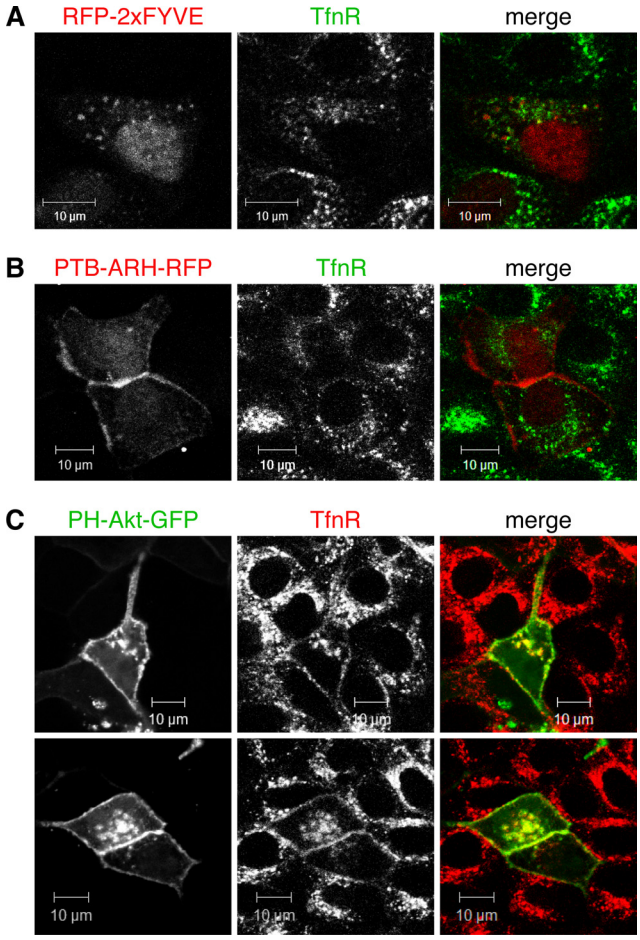

Figure 1. PH-Akt-GFP colocalizes with TfnR. MDCK cells grown on coverslips were transiently transfected with cDNAs encoding RFP-2xFYVE (A), PTB-ARH-RFP (B), or PH-Akt-GFP (C). Six hours after transfection (A) or 24 h after transfection (B and C), cells were fixed and incubated with anti-TfnR antibodies (H68.4) followed by incubation with Alexa 488– or Alexa 594–conjugated secondary antibodies. Specimens were analyzed by confocal microscopy, and representative images are shown. Scale bars, 10 μm.

no colocalization between PTB-ARH-RFP or RFP-2xFYVE and TfnR in recycling endosomes. These data suggest that recycling endosomes in MDCK cells may accumulate primarily PI(3,4,5)P_3.

PI(3,4,5)P_3 Accumulates in Recycling Endosomes of AP-1B–positive Epithelial Cells

So far PI(3,4,5)P_3 has been shown to mainly accumulate at the basolateral plasma membrane with some internal puncta in filter-grown MDCK cells (Gassama-Diagne *et al.*, 2006) and at the leading edge of migrating cells (Devreotes and Janetopoulos, 2003) using the same reporter construct PH-Akt-GFP. Therefore, we sought to confirm the localization of PH-Akt-GFP in recycling endosomes. We coexpressed PH-Akt-GFP with mRFP-tagged cellubrevin. RFP-cellubrevin was shown previously to localize in recycling endosomes in MDCK cells (Fields *et al.*, 2007). As shown in Figure 2A, we observed extensive colocalization between PH-Akt-GFP and RFP-cellubrevin. Furthermore, we tested the localization of the PH-domain of Grp1 tagged with mRFP (RFP-PH-Grp1) relative to PH-Akt-GFP. The diglycine splice variant of PH-Grp1 used in this study binds to both PI(3,4,5)P_3 and Arf6-

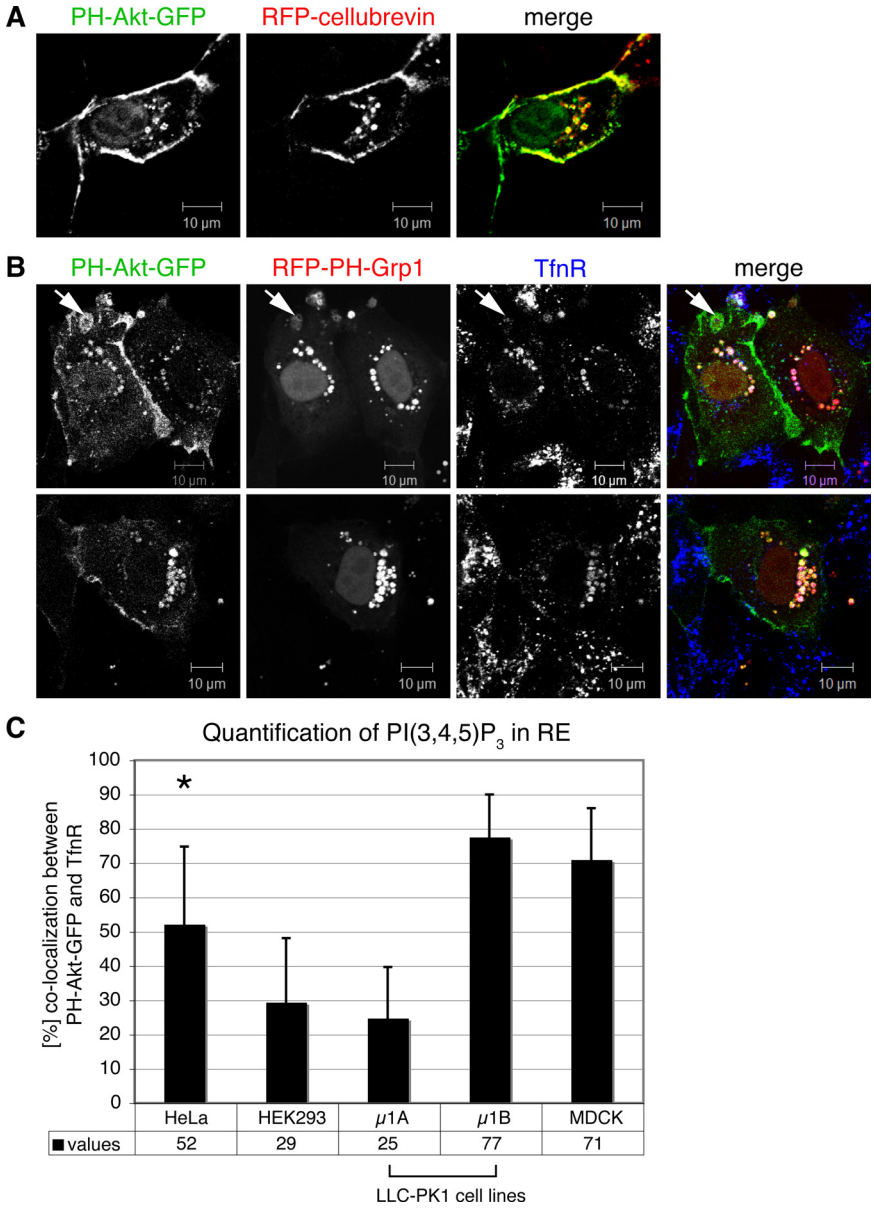

Figure 2. $PI(3,4,5)P_3$ localizes in recycling endosomes. MDCK cells seeded on coverslips were transiently transfected with cDNAs encoding PH-Akt-GFP (A and B), in addition to RFP-cellubrevin (A), or RFP-PH-Grp1 (B). Twenty-four hours after transfection, cells were fixed and incubated with anti-TfnR antibodies (H68.4) followed by incubation with Cy5-labeled secondary antibodies (B). Specimens were analyzed by confocal microscopy and representative images are shown. Scale bars, 10 µm. Arrow in B indicates plasma membrane ruffles. (C) HeLa, HEK293, LLC-PK1::µ1A, LLC-PK1::µ1B, or MDCK cells seeded on coverslips were transfected with cDNA encoding PH-Akt-GFP and stained for TfnR as described in Figure 1. Specimens were analyzed by confocal microscopy, and in cells expressing PH-Akt-GFP the degree of overlap with TfnR in recycling endosomes was analyzed with Volocity software as described in *Materials and Methods.* Data represent mean values of 16 cells (LLC-PK1::µ1A), 21 cells (LLC-PK1::µ1B), 30 cells (HeLa), 40 cells (HEK293), and 35 cells (MDCK). Error bars, SD. Student's unpaired *t* test for all pairwise combinations; statistically significant with $^*p < 0.0001$ or $^*p = 0.0002$ (MDCK vs. HeLa), except for the pairs LLC-PK1::µ1B and MDCK ($p = 0.0955$) as well as LLC-PK1::µ1A and HEK293 ($p = 0.3505$), which showed no statistical significance.

GTP (Di Paolo and De Camilli, 2006; DiNitto *et al.*, 2007). Note, Arf6 localizes in recycling endosomes in MDCK cells (Prigent *et al.*, 2003). Therefore, in MDCK cells the PH domain of Grp1 may localize in recycling endosomes due to interactions with $PI(3,4,5)P_3$ and/or Arf6. We found colocalization of PH-Akt-GFP and RFP-PH-Grp1 in TfnR-positive recycling endosomes and in membrane ruffles at the plasma membrane (Figure 2B).

Taken together, these data demonstrate that indeed recycling endosomes in MDCK cells are positive for $PI(3,4,5)P_3$. This is in contrast to data obtained by other groups in migrating cell lines (Rickert *et al.*, 2000). Therefore we wondered whether $PI(3,4,5)P_3$ accumulation in recycling endosomes is a general feature of epithelial cells. To answer this question we transiently expressed PH-Akt-GFP in a µ1B-negative fibroblast cell line (HEK293), in µ1B-negative epithelial cells (HeLa, LLC-PK1::µ1A), and in µ1B-positive LLC-PK1::µ1B epithelial cells in addition to MDCK cells, which express µ1B endogenously (Ohno *et al.*, 1999). The LLC-PK1 cells are porcine kidney cells that do not express µ1B endogenously (Ohno *et al.*, 1999). These cells were stably transfected with µ1B (LLC-PK1::µ1B) or extra copies of µ1A as control (LLC-PK1::µ1A; Fölsch *et al.*, 1999). Cells were costained for endogenous TfnR and analyzed for colocalization of PH-Akt-GFP and TfnR in perinuclear recycling endosomes using Volocity software as described in *Materials and Methods.* On average, PH-Akt-GFP overlapped to ~50% with TfnR in recycling endosomes in HeLa cells (Figure 2C and Supplemental Figure S1). Note, HeLa cells were heterogeneous with respect to PH-Akt-GFP localization in recycling endosomes. Supplemental Figure S1 depicts two different examples. In HEK293 and LLC-PK1::µ1A cells PH-Akt-GFP localized mainly to the plasma membrane with only ~30 and 25% overlap with TfnR in recycling endosomes, respectively (Figure 2C and Supplemental Figure S1). In contrast, PH-Akt-GFP and TfnR staining overlapped in recycling endosomes to ~75% in LLC-PK1::µ1B and 70% in MDCK cells (Figure 2C and Supplemental Figure S1). The differences between LLC-PK1::µ1B and MDCK cells versus

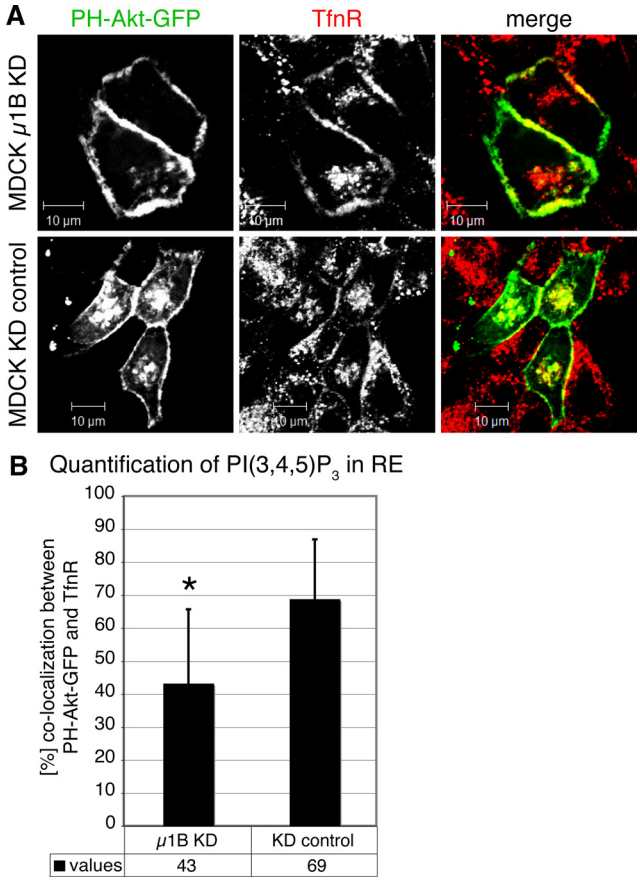

Figure 3. μ1B knockdown in MDCK cells disrupts PH-Akt-GFP localization in recycling endosomes. (A) MDCK cells stably expressing μ1B knockdown shRNA (top) or an empty vector control (bottom) were grown on coverslips and transfected with cDNA encoding PH-Akt-GFP 3 d after seeding. Twenty-four hours later, cells were fixed and stained for endogenous TfnR as described in Figure 1. Specimens were analyzed by confocal microscopy and representative images are shown. Scale bars, 10 μm. (B) For quantification, specimens were further analyzed with Volocity software to determine the degree of overlap between TfnR and PH-Akt-GFP in recycling endosomes of transfected cells as described in *Materials and Methods*. Data represent mean values of 31 cells each. Error bars, SD. Student's unpaired *t* test; *$p < 0.0001$. KD, knockdown.

LLC-PK1::μ1A cells, HEK293, and HeLa cells are statistically significant (cf. figure legends).

Finally, we sought to confirm the relationship between μ1B expression and PI(3,4,5)P_3 accumulation in recycling endosomes with a loss-of-function experiment. We stably knocked down the expression on μ1B with shRNA directed against μ1B in MDCK cells, which was reported to knockdown μ1B expression by >99% and resulted in apical missorting of the AP-1B–dependent cargo NgCAM-CT43 (Anderson *et al.*, 2005). Cells stably transfected with an empty vector served as control. The successful knockdown of μ1B was confirmed by Western blot analysis (not shown). We then transiently expressed PH-Akt-GFP in these cell lines and analyzed the degree of overlap between PH-Akt-GFP and endogenous TfnR in recycling endosomes. We found that the knockdown of μ1B led to a reduction of PH-Akt-GFP localization in recycling endosomes (Figure 3A). The overlap between these two markers was significantly reduced to 43% compared with 69% in the control cells ($p < 0.0001$, cf. figure legends; Figure 3B).

In summary, we found that epithelial cells may accumulate PI(3,4,5)P_3 in recycling endosomes only when μ1B/AP-1B is expressed.

PIPKIγ-90 Localization in Recycling Endosomes Depends on AP-1B Expression

Recently, Ling *et al.* (2007) showed that PIPKIγ-90, the long splice isoform of type Iγ PI(4)P 5-kinase, directly interacts with μ1B via a tyrosine-based motif and partially colocalizes with TfnR in recycling endosomes. In addition, the kinase activity of PIPKIγ-90 was stimulated by μ1B in in vitro assays (Ling *et al.*, 2007). The same kinase was previously described to also bind directly to μ2 of AP-2 and to play a role in PI(4,5)P_2 formation during endocytosis (Bairstow *et al.*, 2006; Krauss *et al.*, 2006). Because the murine PIPKIγ-90 has a total of 661 amino acid residues this splice isoforms is often also referred to as PIPKIγ661 (Ishihara *et al.*, 1998).

To test whether the localization and therefore presumed activity of PIPKIγ-90 in recycling endosomes is linked to μ1B expression, we transiently expressed GFP-PIPKIγ-90 (Di Paolo *et al.*, 2002) in MDCK cells stably expressing shRNA directed against μ1B or control cells and costained for TfnR. We confirmed the partial colocalization of PIPKIγ-90 with TfnR in recycling endosomes (Figure 4A). Importantly, when we analyzed the degree of overlap between GFP-PIPKIγ-90 and TfnR in μ1B knockdown cells, we found a statistically significant reduction from 24 to 10% ($p = 0.0002$, cf. figure legends; Figure 4, A and B). It should be noted that the degree of overlap was quite variable in both control and knockdown cells grown on coverslips. However, whereas ~30% of the control cells showed at least 50% overlap between exogenously expressed GFP-PIPKIγ-90 and TfnR in recycling endosomes, we found this degree of overlap in 0% of μ1B knockdown cells ($p = 0.04$, four independent experiments).

Taken together our data indicate that indeed the partial localization of PIPKIγ-90 in recycling endosomes is facilitated by μ1B/AP-1B expression suggesting that perhaps the kinase activity of PIPKIγ-90 in recycling endosomes might be regulated by AP-1B. This further implies that PI(4,5)P_2 might be an intermediate for PI(3,4,5)P_3 formation at this location.

PI(3,4,5)P_3 Is Necessary for Basolateral Sorting of AP-1B–dependent Cargo

To test whether the accumulation of PI(3,4,5)P_3 is important for the sorting function of recycling endosomes, we manipulated the levels of PI(3,4,5)P_3 in polarized MDCK cells with the PI 3-kinase inhibitor LY294002 and analyzed the sorting behavior of two different cargos. LDLR(Y18A) travels from the TGN to the basolateral membrane without traversing recycling endosomes and does not depend on AP-1B for basolateral sorting. LDLR-CT27 is sorted from the TGN to recycling endosomes for delivery to the basolateral membrane on an AP-1B–dependent pathway (Fields *et al.*, 2007; Nokes *et al.*, 2008). After delivery to the plasma membrane, both receptors are internalized and resorted to the basolateral membrane through recycling endosomes (Matter *et al.*, 1992). During endocytic recycling at steady state again only LDLR-CT27 depends on AP-1B for basolateral delivery (Fields *et al.*, 2007). Fully polarized MDCK cells were infected with defective adenoviruses encoding LDLR(Y18A) or LDLR-CT27. At the time of infection, cells were treated with 50 μM LY294002 or solvent as control (Gassama-Diagne *et al.*, 2006). LY294002 at these concentrations inhibits class I and class II PI 3-kinases as well as PI 4-kinases (Knight *et al.*, 2006). After 48 h the surface pool of LDL

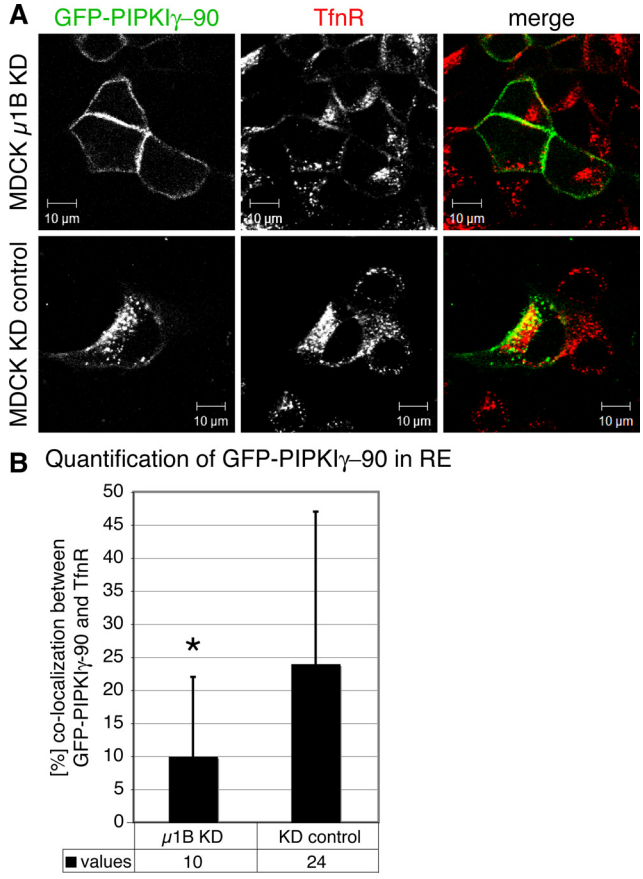

Figure 4. μ1B knockdown in MDCK cells interferes with PIPKIγ-90 localization in recycling endosomes. (A) MDCK cells stably expressing μ1B knockdown shRNA (top) or an empty vector control (bottom) were seeded on coverslips and transiently transfected with plasmids encoding GFP-PIPKIγ-90. Twenty-four hours after transfection, cells were fixed and stained for endogenous TfnR as described in Figure 1. Specimens were analyzed by confocal microscopy and representative images are shown. Scale bars, 10 μm. (B) For quantification, specimens were further analyzed with Volocity software to determine the degree of overlap between TfnR and GFP-PIPKIγ-90 in recycling endosomes of transfected cells as described in *Materials and Methods*. Data represent mean values of 56 knockdown or 44 control cells. Error bars, SD. Student's unpaired *t* test; *p = 0.0002. KD, knockdown.

receptors was immunolabeled with antibodies recognizing their ectodomain to determine their polarized distribution. As shown in Figure 5A, treatment of MDCK cells with 50 μM LY294002 led to apical missorting of LDLR-CT27 in ~95% of cells analyzed (Figure 5, A and C). Importantly, LDLR(Y18A) was still sorted correctly indicating that membrane trafficking from the TGN to the basolateral membrane or correct endocytic recycling from early endosomes back to the basolateral membrane was not disturbed by LY294002 treatment (Figure 5A). Rather, LY294002 treatment seems to specifically inhibit basolateral sorting of LDLR-CT27 from recycling endosomes. In agreement with the sorting data, we found that treatment with LY294002 disrupted costaining of PH-Akt-GFP with TfnR in recycling endosomes, but not PH-Akt-GFP localization at the plasma membrane in coverslip-grown MDCK cells (Supplemental Figure S2A). These data show that LY294002 was effective in preventing $PI(3,4,5)P_3$ formation in recycling endosomes. Notably, the staining for TfnR in this experiment seems more dispersed after treatment with LY294002 consistent with previous findings showing that treatment of HeLa cells with 100 μM LY294002 led to an accumulation of TfnR in early endosomes most likely because of a decrease in the rate of fast recycling from early endosomes to the plasma membrane (van Dam *et al.*, 2002). The previous study further showed that endocytosis and trafficking into and out of recycling endosomes was not affected by LY294002 treatment (van Dam *et al.*, 2002). LLC-PK1 cells did not tolerate LY29402 treatment well, and we were thus unable to determine the consequences of LY294002 treatment on AP-1B localization in LLC-PK1 cells stably expressing HA-tagged μ1B. Regardless, these data suggest that $PI(3,4,5)P_3$ formation in recycling endosomes may be important for basolateral sorting of LDLR-CT27.

Because we used LY294002 at concentrations that also inhibit PI 4-kinases, we sought to manipulate $PI(3,4,5)P_3$ levels in the cells with the lipid phosphatase PTEN, which specifically dephosphorylates $PI(3,4,5)P_3$ to $PI(4,5)P_2$ (Downes *et al.*, 2001; Di Paolo and De Camilli, 2006). We transiently coexpressed LDLR(Y18A) or LDLR-CT27 with T7-tagged PTEN in fully polarized MDCK cells. Twenty-four hours after transfection, LDLR at the surface was labeled with antibodies recognizing its ectodomain as before (note: both anti-LDLR and anti-T7 antibodies were of the same isotype, therefore LDLR at the surface is doubly stained; cf. figure legends). Remarkably, we observed missorting of LDLR-CT27 to the apical plasma membrane domain in virtually 100% of cells analyzed coexpressing PTEN (Figure 5, B and C). In contrast, LDLR(Y18A) was not missorted at all when coexpressed with PTEN again indicating that PTEN overexpression does not disrupt the overall polarity, delivery of LDLR(Y18A) from the TGN to the plasma membrane or endocytic recycling from early endosomes in this assay (Figure 5B). Moreover, overexpression of PTEN in coverslip-grown MDCK cells led to a displacement of PH-Akt-GFP from recycling endosomes and the plasma membrane indicating that $PI(3,4,5)P_3$ was indeed lost from these compartments (Supplemental Figure S2B).

$PI(3,4,5)P_3$ Is Needed to Recruit AP-1B onto Recycling Endosomes

Next, we directly tested whether overexpression of PTEN had any effects on AP-1B localization. Because no antibodies exist for immunofluorescence that distinguish between μ1A and μ1B, we transiently expressed T7-PTEN in LLC-PK1 cells stably expressing HA-tagged μ1B (LLC-PK1::μ1B-HA) as well as in LLC-PK1 cells stably expressing HA-tagged μ1A (LLC-PK1::μ1A-HA) as controls (Fölsch *et al.*, 2001). As was the case with MDCK cells (Supplemental Figure S2B), PTEN overexpression led to a disruption of perinuclear staining of PH-Akt-GFP in LLC-PK1::μ1B-HA cells (not shown), indicating that LLC-PK1::μ1B cells behave similarly to MDCK cells. In addition to PTEN, human TfnR was coexpressed and before fixation, cells were allowed to take up Alexa 488–labeled human Tfn to visualize the recycling endosomes. The fact that we observe Tfn uptake into recycling endosomes in the presence of PTEN argues that the early endocytic pathway is not disrupted by PTEN expression and AP-1B cargo is present in recycling endosomes. Importantly, AP-1B-HA became displaced from Tfn-positive recycling endosomes in PTEN-expressing cells (Figure 6, bottom), but not in neighboring cells not expressing PTEN. Loss of AP-1B localization in recycling endosomes is statistically significant ($p < 0.0001$) and was observed in 91 ± 9% of PTEN-expressing cells (Figure 6).

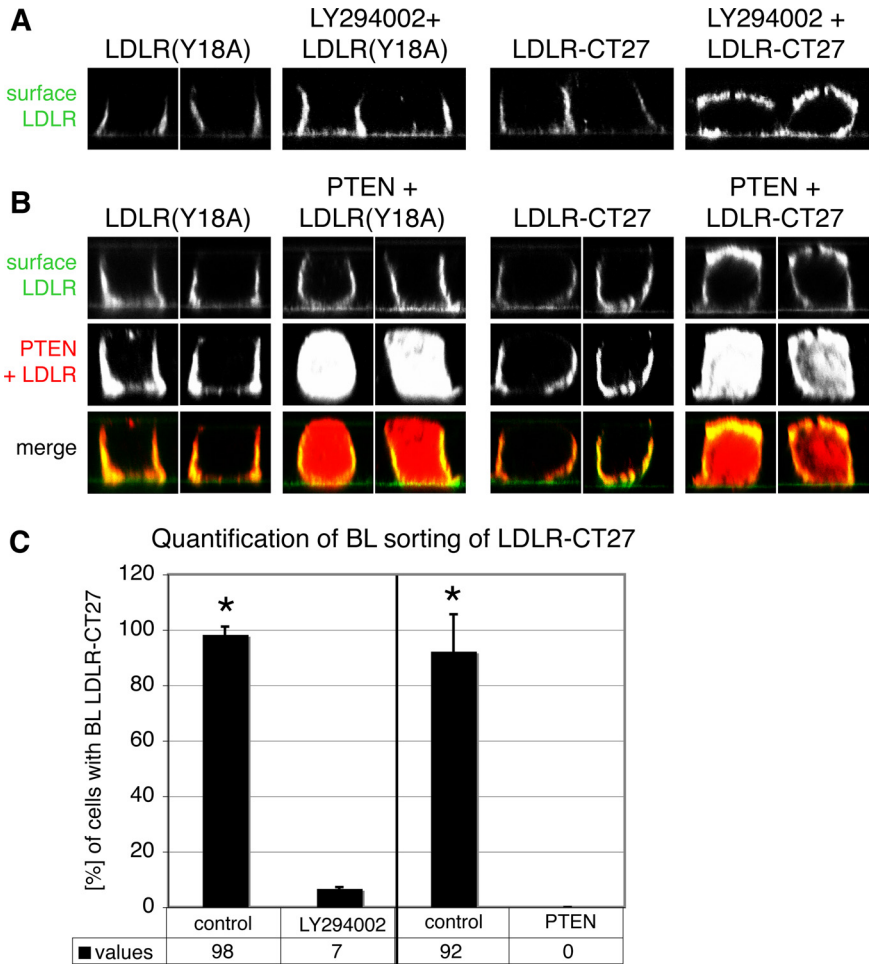

Figure 5. PI(3,4,5)P_3 is necessary for basolateral sorting of LDLR-CT27. (A) MDCK cells grown on filter supports for 3 d were infected with defective adenoviruses encoding LDLR (Y18A) (left panels) or LDLR-CT27 (right panels). During infection, cells were simultaneously treated with 50 μM LY294002. Forty-eight hours after infection and after treatment, cells were incubated with anti-LDLR (C7) antibodies to stain LDLR at the surface. Cells were then fixed and incubated with Alexa 488–labeled secondary antibodies. (B) MDCK cells seeded on filters were transfected with cDNAs encoding T7-PTEN and either LDLR(Y18A) (left panels) or LDLR-CT27 (right panels). Twenty-four hours after transfection, cells were incubated with anti-LDLR (C7, mouse IgG2b) antibodies to stain LDLR at the surface. Cells were then fixed and incubated with Alexa 488–labeled secondary antibodies. Cells were subsequently fixed again, permeabilized, and incubated with anti-T7 antibodies (mouse IgG2b) to stain for T7-PTEN internally. Subsequently, cells were incubated with Alexa 594–labeled secondary antibodies against mouse IgG2b, which recognize both anti-T7 and anti-LDLR primary antibodies explaining the Alexa 594 staining of surface LDLR. (A and B) Specimens were analyzed by confocal microscopy and representative XZ-sections are shown. (C) For quantification, MDCK cells treated with LY294002 or MDCK cells coexpressing LDLR-CT27 and T7-PTEN as well as the respective control cells were scored whether or not LDLR-CT27 was localized exclusively at the basolateral membrane or missorted to the apical membrane. Data represent mean values from three independent experiments counting at least 35 cells per condition. Error bars, SD. Student's unpaired *t* test for pairwise combinations of treatment (LY294002 or PTEN) and appropriate mock treatment control; *$p < 0.0001$. BL, basolateral.

In contrast, AP-1A-HA was not displaced by PTEN overexpression, suggesting differential dependencies of AP-1A and AP-1B toward PI(3,4,5)P_3 (Figure 6, top, only 8 ± 10% of the LLC-PK1::μ1A-HA cells analyzed showed loss of perinuclear localization of AP-1A).

In summary, our data demonstrate that PI(3,4,5)P_3 accumulation in recycling endosomes is important for AP-1B recruitment to this compartment (Figure 6) and subsequent basolateral sorting of AP-1B–dependent cargo (Figure 5).

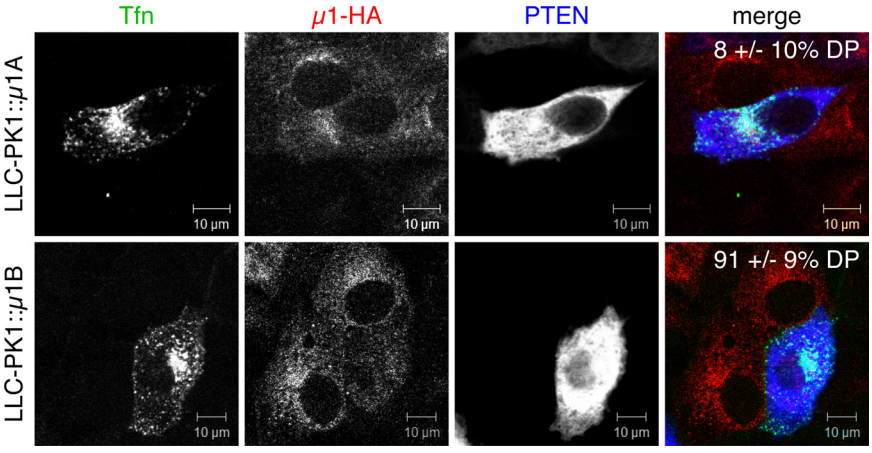

Figure 6. PI(3,4,5)P_3 is needed for membrane recruitment of AP-1B. LLC-PK1::μ1A-HA (top) or LLC-PK1::μ1B-HA (bottom) cells seeded on coverslips were transfected with cDNAs encoding T7-PTEN and human TfnR. Twenty-four hours after transfection cells were serum-starved and allowed to uptake Alexa 488–labeled human Tfn as described in *Materials and Methods*. Cells were then fixed and incubated with anti-HA (mouse IgG1) and anti-T7 (mouse IgG2b) antibodies. Subsequently, specimens were incubated with Alexa 594–labeled goat anti-mouse IgG1 antibodies and Cy5-labeled goat anti-mouse IgG2b antibodies. Specimens were analyzed by confocal microscopy, and representative images are shown. Scale bars, 10 μm. For quantification, cells coexpressing T7-PTEN and AP-1A-HA or AP-1B-HA were scored for perinuclear localization of AP-1A-HA (30 cells) or AP-1B-HA (46 cells), respectively. Data represent mean values of four independent experiments; errors bars, SD. Student's unpaired *t* test; $p < 0.0001$. DP, disruption phenotype.

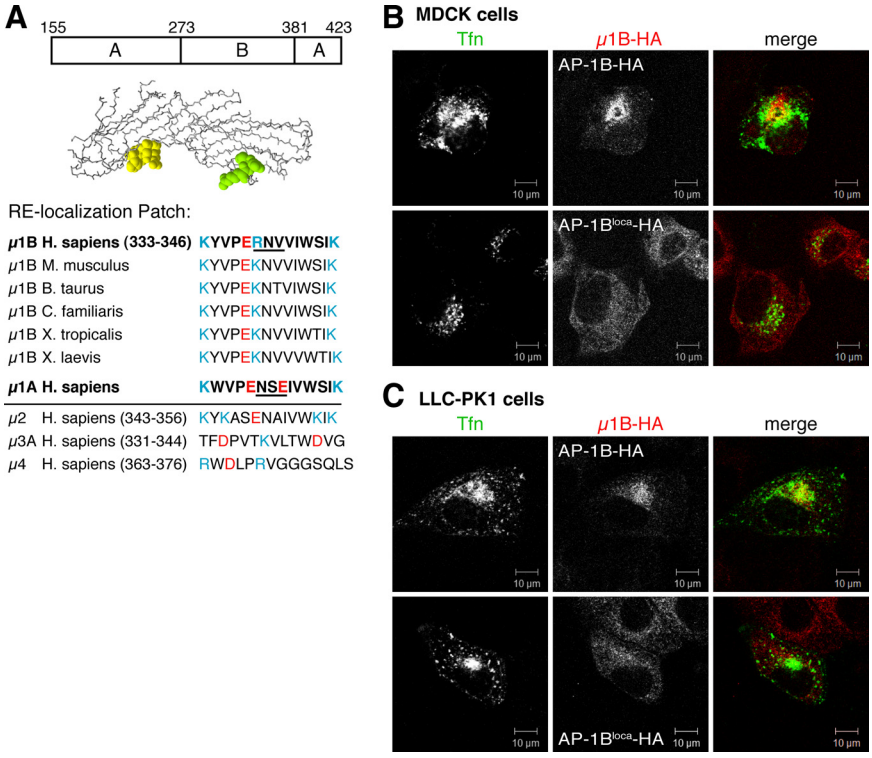

Figure 7. A patch of three amino acid residues in μ1B is necessary for AP-1B localization. (A) Schematic diagram of the C-terminus of μ1B and model of the C-terminus of μ1B threaded according to the atomic structure of μ2 using Swiss-Pdb Viewer (DeepView) software (www.expasy.org/spdbv; Guex and Peitsch, 1997). Residues highlighted in yellow are involved in cargo binding, and residues highlighted in green are residues important for membrane recruitment of AP-1B. Amino acid residues of the putative membrane-recruitment patch show regions of high similarity across species for μ1B and dissimilarity in other μ subunits. In this region, basic residues are shown in blue and acidic residues in red. Site-directed mutagenesis was used to replace residues in μ1B with corresponding residues from μ1A (underlined residues). (B) MDCK cells were seeded on collagen/fibronectin-coated coverslips and transiently transfected with cDNAs encoding μ1B-HA (top) or μ1B^{loca}-HA (bottom) and human TfnR. (C) LLC-PK1::μ1B-HA (top) and LLC-PK1::μ1B^{loca}-HA (bottom) cell lines were seeded on coverslips and transiently transfected with cDNA encoding human TfnR. (B and C) Twenty-four hours after transfection, cells were serum-starved and allowed to uptake Alexa 488–labeled human Tfn as described in *Materials and Methods.* Cells were then fixed and incubated with anti-HA antibodies. Subsequently, samples were incubated with Alexa 594–labeled secondary antibodies. Specimens were analyzed by confocal microscopy and representative images are shown. Scale bars, 10 μm. RE, recycling endosomes.

A Patch of Three Amino Acid Residues in μ1B Is Needed for AP-1B Recruitment onto Recycling Endosomes

To better understand the differences in membrane recruitment between AP-1A and AP-1B, we examined in more detail the C-terminus of μ1B. Based on crystal structures, the C-termini of adaptor μ chains contain two subdomains (Owen and Evans, 1998; Heldwein *et al.*, 2004). The more N-terminally positioned subdomain A (amino acids 155-272 and 382-423 in μ1) is mainly involved in forming the binding pocket for the tyrosine-based sorting signals (Owen and Evans, 1998). The second, C-terminal subdomain B of μ2 is involved in binding to PI(4,5)P_2. Subdomain B corresponds to amino acids 273-381 in μ1 (Collins *et al.*, 2002; Figure 7A). In contrast, the N-terminus of the μ chain is needed for its incorporation into the AP complex (Collins *et al.*, 2002; Heldwein *et al.*, 2004).

Guided by the published lipid-binding patch of μ2 (Collins *et al.*, 2002), we reasoned amino acid residues 333-346 might be involved in membrane recruitment of μ1B/AP-1B. Alignment of these residues showed that this patch is extremely well conserved among μ1B homologues from different species. However, this patch is not at all conserved among other adaptor complex μ chains (Figure 7A). Notably, μ1B has an additional positive charge in the middle of this region, which is not found in μ1A. Conversely, μ1A has a negative charge in the middle of this region that is not present in μ1B. To create a putative membrane-recruitment mutant, we mutated R338, N339, and V340 in HA-tagged μ1B (μ1B-HA) into the corresponding residues present in μ1A (R338N/N339S/V340E) to create HA-tagged μ1B^{loca} (μ1B^{loca}-HA). The R338N/N339S/V340E mutation in μ1B^{loca} changed the net charge of amino acids 333-346 from +2 to 0 (Figure 7A). We reasoned that exchanging residues in μ1B with those present in μ1A should not interfere with the folding of μ1B.

Next, we cotransfected cDNAs encoding μ1B-HA or μ1B^{loca}-HA together with cDNA encoding human TfnR into MDCK cells. Whereas μ1B-HA/AP-1B-HA colocalized with internalized human Tfn as expected, μ1B^{loca}-HA/AP-1B^{loca}-HA failed to specifically localize in recycling endosomes and instead was found more randomly dispersed in these cells (Figure 7B). In addition, we stably expressed μ1B-HA and μ1B^{loca}-HA in LLC-PK1 cells (LLC-PK1::μ1B-HA and LLC-PK1::μ1B^{loca}-HA). Using LLC-PK1 cells has the added benefit, that they do not express endogenous μ1B (Ohno *et al.*, 1999). Therefore, the exogenously expressed form of μ1B is the only form of μ1B present in the cells. As described previously, μ1B-HA stably expressed in LLC-PK1 cells incorporates into AP-1 complexes and rescues LDLR missorting (Fölsch *et al.*, 2001). Stable cell lines were subjected to Western blot analysis to test for expression levels of μ1B-HA relative to total μ1A and γ-adaptin. We found that LLC-PK1::μ1B-HA and LLC-PK1::μ1B^{loca}-HA cell lines expressed comparable amounts of HA-tagged μ1B, which was increased about two- to fivefold over endogenous μ1A (Supplemental Figure S3A). In addition, μ1B^{loca}-HA coprecipitated with the large AP-1 subunit γ-adaptin, indicating successful incorporation of μ1B^{loca}-HA into AP-1B^{loca}-HA complexes (Supplemental Figure S3B). As shown previously, we detected partial costaining for AP-1B-HA and Tfn (Figure 7C; Fölsch *et al.*, 2001). In contrast, AP-1B^{loca}-HA failed again to localize specifically in recycling endosomes (Figure 7C). Unfortunately, LLC-PK1::μ1B^{loca}-HA cells did not polarize well on filter supports (S.M.K. and H.F., unpublished observation), preventing us from analyzing LDLR-CT27 sorting in this cell line. However, AP-1B^{loca}-HA did not interfere with accumulation

of Tfn in recycling endosomes (Figure 7C) or VSVG trafficking to the cell surface in nonpolarized cells during a 2-h chase period (Supplemental Figure S3C), indicating that expression of localization-impaired AP-1B has no inhibitory effect on general intracellular trafficking pathways. Furthermore, the intracellular localization of cation-independent mannose 6-phosphate receptor (CI-MPR) or TGN38, a marker protein for the TGN, were also largely unaffected in LLC-PK1::μ1B^{loca}-HA cells (Supplemental Figure S3, D and E), further suggesting that AP-1A function may not be impaired by AP-1B^{loca}-HA expression. Note, TGN38 was shown previously to colocalize with AP-1A at the TGN, whereas CI-MPR partially colocalizes with both AP-1A and AP-1B and copurified with AP-1B vesicles indicating that in epithelial cells AP-1B is involved in steady-state localization of CI-MPR, perhaps explaining a slightly more diffuse staining of the CI-MPR in LLC-PK1::μ1B^{loca} cells (Fölsch *et al.*, 2003). Finally, we tested whether the C-terminus of μ1B could be recruited onto PI(3,4,5)P_3-containing liposomes in vitro, but did not observe robust recruitment (not shown). Regardless, data obtained by expressing AP-1B^{loca}-HA in MDCK and LLC-PK1 cells show that only a few amino acid residues in the C-terminus of μ1B are crucial for correct membrane recruitment of AP-1B.

Taken together, we found by two independent assays that mutations in the putative membrane-recruitment patch of μ1B interferes with the localization of AP-1B in recycling endosomes.

DISCUSSION

Even though it has been well established that polarized epithelial cells express two biochemically and functionally distinct AP-1 complexes that localize to different membrane compartments, the molecular nature of this different localization was not known (Fölsch, 2005). In this study we identify a membrane-recruitment patch in the C-terminus of the medium subunit μ1B of AP-1B that is essential for localization of AP-1B in recycling endosomes. A second major finding in this study is that epithelial cells expressing AP-1B accumulate PI(3,4,5)P_3 in recycling endosomes, which is essential for AP-1B localization and function.

Based on biochemical and crystal structure data gained from both AP-2 and AP-1A, adaptor complexes are thought to undergo conformational changes during membrane recruitment (Collins *et al.*, 2002; Heldwein *et al.*, 2004). In the cytosol, the C-terminus of the medium subunit is folded back onto the complex. On membrane recruitment, however, a linker in the medium subunit is phosphorylated which is believed to result in a conformational change that exposes the C-terminus to the cytosol and allows for cargo and membrane lipid binding (Kirchhausen, 2002). Based on the similarities between AP-1A and AP-1B, it is likely that the C-terminus of μ1B is also exposed during membrane recruitment and may therefore be involved in specific protein–protein or protein–lipid interactions. The putative membrane-recruitment patch in μ1B is located in a cluster of basic and hydrophobic amino acid residues (333-346), corresponding to amino acid residues that have been described in μ2 to bind to PI(4,5)P_2 (Collins *et al.*, 2002). In μ1B this patch is clearly necessary for membrane recruitment of μ1B/AP-1B and the mutant complex AP-1B^{loca} failed to localize correctly. Because we reverted residues in μ1B to those present in μ1A, these data also show that changing three amino acid residues in μ1B is not sufficient to revert localization of AP-1B^{loca} to the TGN. Presumably, additional residues in μ1A not present in μ1B^{loca} are needed for TGN localization. We also found that AP-1B^{loca} largely did not interfere with intracellular localizations of TGN38 and CI-MPR or VSVG and TfnR trafficking in nonpolarized cells. However, AP-1B^{loca} seems to act as a dominant-negative protein complex for cell polarization, because LLC-PK1::μ1B^{loca}-HA cells did not polarize well on filter supports. This might be explained by the fact that functions of AP-1B in exocyst recruitment, for example, (Fölsch *et al.*, 2003) may still be functional in AP-1B^{loca}.

In addition to the patch of three amino acid residues mutated in μ1B^{loca}, we identified PI(3,4,5)P_3 as another necessary component for stable membrane recruitment of AP-1B. Recent evidence had implicated PI(3,4,5)P_3 and PI(4,5)P_2 in playing important roles in organization of the basolateral and apical plasma membrane domains, respectively, during formation of AP-1B–positive epithelial cysts (Gassama-Diagne *et al.*, 2006; Kierbel *et al.*, 2007; Martin-Belmonte *et al.*, 2007). Using multiple probes that recognize PI(3,4,5)P_3 (PH-Akt, PH-Grp1) in combination with probes recognizing recycling endosomes (TfnR, cellubrevin) we made the important observation that recycling endosomes are enriched in PI(3,4,5)P_3. In the future it will be interesting to learn if the accumulation of PI(3,4,5)P_3 in recycling endosomes is dependent on cell polarization. The importance of PI(3,4,5)P_3 is highlighted by the fact that overexpression of the PI(3,4,5)P_3-specific phosphatase PTEN leads to a displacement of AP-1B from recycling endosomes and apical missorting of AP-1B–dependent cargo. These data suggest that AP-1B may associate primarily with PI(3,4,5)P_3-positive membranes in vivo. μ1B/AP-1B may either bind to an as yet not characterized protein that requires PI(3,4,5)P_3 for localization in recycling endosomes or μ1B may directly bind PI(3,4,5)P_3. Regardless, we identified a membrane-recruitment patch in μ1B, and future experiments are aimed at elucidating how this patch regulates AP-1B recruitment to PI(3,4,5)P_3-positive membranes.

Another major finding is that AP-1B expression itself is necessary for PI(3,4,5)P_3 accumulation in recycling endosomes. The main question that arises then is how AP-1B influences lipid metabolism. To generate PI(3,4,5)P_3, phosphoinositides have to be phosphorylated at the positions 3, 4, and 5. Because the TGN is enriched in PI(4)P (Roth, 2004) and there is considerable membrane trafficking from the TGN into recycling endosomes (Ang *et al.*, 2004; Fields *et al.*, 2007; Gravotta *et al.*, 2007), it seems reasonable to assume that PI(4)P might be the starting lipid for PI(3,4,5)P_3 formation in recycling endosomes. To generate PI(3,4,5)P_3, we postulate the cooperative actions of PI(4)P 5-kinases and PI 3-kinases. Perhaps AP-1B is initially recruited onto recycling endosomes by a loose association of the γ-subunit to PI(4)P during polarization (Heldwein *et al.*, 2004). Subsequently, AP-1B or components of the clathrin coat may orchestrate PI(3,4,5)P_3 formation to stabilize AP-1B's association with recycling endosomes by recruiting lipid kinases. In agreement with this hypothesis, we show that the partial localization of the PI(4)P 5-kinase PIPKIγ-90 in recycling endosomes is facilitated by AP-1B expression. Because it was shown that μ1B/AP-1B stimulates the kinase activity of PIPKIγ-90 (Ling *et al.*, 2007), this finding suggests that PI(3,4,5)P_3 formation in recycling endosomes may involve PI(4,5)P_2 as an intermediate.

To generate PI(3,4,5)P_3 from PI(4)P we further postulate the involvement of a PI 3-kinase. A good candidate is the class II PI 3-kinase C2α (PI3K-C2α). This kinase binds directly to clathrin (Gaidarov *et al.*, 2001) and was described to localize to both plasma membrane and TGN (Domin *et al.*, 2000). Perhaps HeLa cells maintain some functional aspects

of PI(3,4,5)P_3 formation accounting for the relatively high extent (~50%) of PI(3,4,5)P_3 localization we observed in recycling endosomes of μ1B-negative HeLa cells.

In the future it will be important to explore the relationship between AP-1B expression and PI(3,4,5)P_3 accumulation in recycling endosomes and the consequences this might have on cell homeostasis, AP-1B vesicle formation, polarity maintenance, and signaling.

ACKNOWLEDGMENTS

We are indebted to Drs. Pietro De Camilli, Peter Devreotes, Sandra Maday, Ira Mellman, Suzanne Pfeffer, Linton Traub, and Graham Warren for the gift of reagents. In addition, we are grateful to Dr. Bettina Winckler (University of Virginia, Charlottesville, VA) for comments on the manuscript. This work was funded by a grant from the National Institutes of Health (GM070736) to H.F. and was supported in part by a Katten Muchin Rosenman Travel Scholarship Award from the Robert H. Lurie Comprehensive Cancer Center of Northwestern University to S.M.K. R.S.K. was supported by the Cellular and Molecular Basis of Disease Training Program (GM8061).

REFERENCES

Anderson, E., Maday, S., Sfakianos, J., Hull, M., Winckler, B., Sheff, D., Fölsch, H., and Mellman, I. (2005). Transcytosis of NgCAM in epithelial cells reflects differential signal recognition on the endocytic and secretory pathways. J. Cell Biol. *170*, 595–605.

Ang, A. L., Taguchi, T., Francis, S., Fölsch, H., Murrells, L. J., Pypaert, M., Warren, G., and Mellman, I. (2004). Recycling endosomes can serve as intermediates during transport from the Golgi to the plasma membrane of MDCK cells. J. Cell Biol. *167*, 531–543.

Bairstow, S. F., Ling, K., Su, X., Firestone, A. J., Carbonara, C., and Anderson, R. A. (2006). Type Igamma661 phosphatidylinositol phosphate kinase directly interacts with AP2 and regulates endocytosis. J. Biol. Chem. *281*, 20632–20642.

Brodsky, F. M., Chen, C. Y., Knuehl, C., Towler, M. C., and Wakeham, D. E. (2001). Biological basket weaving: formation and function of clathrin-coated vesicles. Annu. Rev. Cell Dev. Biol. *17*, 517–568.

Collins, B. M., McCoy, A. J., Kent, H. M., Evans, P. R., and Owen, D. J. (2002). Molecular architecture and functional model of the endocytic AP2 complex. Cell *109*, 523–535.

Devreotes, P., and Janetopoulos, C. (2003). Eukaryotic chemotaxis: distinctions between directional sensing and polarization. J. Biol. Chem. *278*, 20445–20448.

Di Paolo, G., and De Camilli, P. (2006). Phosphoinositides in cell regulation and membrane dynamics. Nature *443*, 651–657.

Di Paolo, G., Pellegrini, L., Letinic, K., Cestra, G., Zoncu, R., Voronov, S., Chang, S., Guo, J., Wenk, M. R., and De Camilli, P. (2002). Recruitment and regulation of phosphatidylinositol phosphate kinase type 1 gamma by the FERM domain of talin. Nature *420*, 85–89.

DiNitto, J. P., Delprato, A., Gabe Lee, M. T., Cronin, T. C., Huang, S., Guilherme, A., Czech, M. P., and Lambright, D. G. (2007). Structural basis and mechanism of autoregulation in 3-phosphoinositide-dependent Grp1 family Arf GTPase exchange factors. Mol. Cell *28*, 569–583.

Domin, J., Gaidarov, I., Smith, M. E., Keen, J. H., and Waterfield, M. D. (2000). The class II phosphoinositide 3-kinase PI3K-C2alpha is concentrated in the trans-Golgi network and present in clathrin-coated vesicles. J. Biol. Chem. *275*, 11943–11950.

Downes, C. P., Bennett, D., McConnachie, G., Leslie, N. R., Pass, I., MacPhee, C., Patel, L., and Gray, A. (2001). Antagonism of PI 3-kinase-dependent signalling pathways by the tumour suppressor protein, PTEN. Biochem. Soc. Trans. *29*, 846–851.

Fields, I. C., Shteyn, E., Pypaert, M., Proux-Gillardeaux, V., Kang, R. S., Galli, T., and Fölsch, H. (2007). v-SNARE cellubrevin is required for basolateral sorting of AP-1B-dependent cargo in polarized epithelial cells. J. Cell Biol. *177*, 477–488.

Fölsch, H. (2005). The building blocks for basolateral vesicles in polarized epithelial cells. Trends Cell Biol. *15*, 222–228.

Fölsch, H. (2008). Regulation of membrane trafficking in polarized epithelial cells. Curr. Opin. Cell Biol. *20*, 208–213.

Fölsch, H., Ohno, H., Bonifacino, J. S., and Mellman, I. (1999). A novel clathrin adaptor complex mediates basolateral targeting in polarized epithelial cells. Cell *99*, 189–198.

Fölsch, H., Pypaert, M., Maday, S., Pelletier, L., and Mellman, I. (2003). The AP-1A and AP-1B clathrin adaptor complexes define biochemically and functionally distinct membrane domains. J. Cell Biol. *163*, 351–362.

Fölsch, H., Pypaert, M., Schu, P., and Mellman, I. (2001). Distribution and function of AP-1 clathrin adaptor complexes in polarized epithelial cells. J. Cell Biol. *152*, 595–606.

Gaidarov, I., Smith, M. E., Domin, J., and Keen, J. H. (2001). The class II phosphoinositide 3-kinase C2alpha is activated by clathrin and regulates clathrin-mediated membrane trafficking. Mol. Cell *7*, 443–449.

Gan, Y., McGraw, T. E., and Rodriguez-Boulan, E. (2002). The epithelial-specific adaptor AP1B mediates post-endocytic recycling to the basolateral membrane. Nat. Cell Biol. *4*, 605–609.

Gassama-Diagne, A., Yu, W., ter Beest, M., Martin-Belmonte, F., Kierbel, A., Engel, J., and Mostov, K. (2006). Phosphatidylinositol-3,4,5-trisphosphate regulates the formation of the basolateral plasma membrane in epithelial cells. Nat. Cell Biol. *8*, 963–970.

Gillooly, D. J., Morrow, I. C., Lindsay, M., Gould, R., Bryant, N. J., Gaullier, J. M., Parton, R. G., and Stenmark, H. (2000). Localization of phosphatidylinositol 3-phosphate in yeast and mammalian cells. EMBO J. *19*, 4577–4588.

Gravotta, D., Deora, A., Perret, E., Oyanadel, C., Soza, A., Schreiner, R., Gonzalez, A., and Rodriguez-Boulan, E. (2007). AP1B sorts basolateral proteins in recycling and biosynthetic routes of MDCK cells. Proc. Natl. Acad. Sci. USA *104*, 1564–1569.

Guex, N., and Peitsch, M. C. (1997). SWISS-MODEL and the Swiss-Pdb-Viewer: an environment for comparative protein modeling. Electrophoresis *18*, 2714–2723.

Heldwein, E. E., Macia, E., Wang, J., Yin, H. L., Kirchhausen, T., and Harrison, S. C. (2004). Crystal structure of the clathrin adaptor protein 1 core. Proc. Natl. Acad. Sci. USA *101*, 14108–14113.

Hirst, J., and Robinson, M. S. (1998). Clathrin and adaptors. Biochim. Biophys. Acta *1404*, 173–193.

Ishihara, H., Shibasaki, Y., Kizuki, N., Wada, T., Yazaki, Y., Asano, T., and Oka, Y. (1998). Type I phosphatidylinositol-4-phosphate 5-kinases. Cloning of the third isoform and deletion/substitution analysis of members of this novel lipid kinase family. J. Biol. Chem. *273*, 8741–8748.

James, S. R., Downes, C. P., Gigg, R., Grove, S. J., Holmes, A. B., and Alessi, D. R. (1996). Specific binding of the Akt-1 protein kinase to phosphatidylinositol 3,4,5-trisphosphate without subsequent activation. Biochemical J. *315*(Pt 3), 709–713.

Kierbel, A., Gassama-Diagne, A., Rocha, C., Radoshevich, L., Olson, J., Mostov, K., and Engel, J. (2007). Pseudomonas aeruginosa exploits a PIP3-dependent pathway to transform apical into basolateral membrane. J. Cell Biol. *177*, 21–27.

Kirchhausen, T. (2002). Clathrin adaptors really adapt. Cell *109*, 413–416.

Knight, Z. A., *et al.* (2006). A pharmacological map of the PI3-K family defines a role for p110alpha in insulin signaling. Cell *125*, 733–747.

Krauss, M., Kukhtina, V., Pechstein, A., and Haucke, V. (2006). Stimulation of phosphatidylinositol kinase type I-mediated phosphatidylinositol (4,5)-bisphosphate synthesis by AP-2mu-cargo complexes. Proc. Natl. Acad. Sci. USA *103*, 11934–11939.

Ling, K., Bairstow, S. F., Carbonara, C., Turbin, D. A., Huntsman, D. G., and Anderson, R. A. (2007). Type Igamma phosphatidylinositol phosphate kinase modulates adherens junction and E-cadherin trafficking via a direct interaction with micro1B adaptin. J. Cell Biol. *176*, 343–353.

Manders, E.M.M., Verbeek, F. J., and Aten, J. A. (1993). Measurement of co-localization of objects in dual-color confocal images. J. Microsc. *169*, 375–382.

Martin-Belmonte, F., Gassama, A., Datta, A., Yu, W., Rescher, U., Gerke, V., and Mostov, K. (2007). PTEN-mediated apical segregation of phosphoinositides controls epithelial morphogenesis through Cdc42. Cell *128*, 383–397.

Matter, K., Hunziker, W., and Mellman, I. (1992). Basolateral sorting of LDL receptor in MDCK cells: the cytoplasmic domain contains two tyrosine-dependent targeting determinants. Cell *71*, 741–753.

Mostov, K., Su, T., and ter Beest, M. (2003). Polarized epithelial membrane traffic: conservation and plasticity. Nat. Cell Biol. *5*, 287–293.

Nakatsu, F., and Ohno, H. (2003). Adaptor protein complexes as the key regulators of protein sorting in the post-Golgi network. Cell. Struct. Funct. *28*, 419–429.

Nokes, R. L., Fields, I. C., Collins, R. N., and Fölsch, H. (2008). Rab13 regulates membrane trafficking between TGN and recycling endosomes in polarized epithelial cells. J. Cell Biol. *182*, 845–853.

Ohno, H., Tomemori, T., Nakatsu, F., Okazaki, Y., Aguilar, R. C., Fölsch, H., Mellman, I., Saito, T., Shirasawa, T., and Bonifacino, J. S. (1999). Mu1B, a novel adaptor medium chain expressed in polarized epithelial cells. FEBS Lett. *449*, 215–220.

Owen, D. J., and Evans, P. R. (1998). A structural explanation for the recognition of tyrosine-based endocytotic signals. Science *282*, 1327–1332.

Paleotti, O., Macia, E., Luton, F., Klein, S., Partisani, M., Chardin, P., Kirchhausen, T., and Franco, M. (2005). The small G-protein Arf6GTP recruits the AP-2 adaptor complex to membranes. J. Biol. Chem. *280*, 21661–21666.

Prigent, M., Dubois, T., Raposo, G., Derrien, V., Tenza, D., Rosse, C., Camonis, J., and Chavrier, P. (2003). ARF6 controls post-endocytic recycling through its downstream exocyst complex effector. J. Cell Biol. *163*, 1111–1121.

Rickert, P., Weiner, O. D., Wang, F., Bourne, H. R., and Servant, G. (2000). Leukocytes navigate by compass: roles of PI3Kgamma and its lipid products. Trends Cell Biol. *10*, 466–473.

Robinson, M. S., and Bonifacino, J. S. (2001). Adaptor-related proteins. Curr. Opin. Cell Biol. *13*, 444–453.

Rodriguez-Boulan, E., Kreitzer, G., and Musch, A. (2005). Organization of vesicular trafficking in epithelia. Nat. Rev. *6*, 233–247.

Roth, M. G. (2004). Phosphoinositides in constitutive membrane traffic. Physiol. Rev. *84*, 699–730.

van Dam, E. M., Ten Broeke, T., Jansen, K., Spijkers, P., and Stoorvogel, W. (2002). Endocytosed transferrin receptors recycle via distinct dynamin and phosphatidylinositol 3-kinase-dependent pathways. J. Biol. Chem. *277*, 48876–48883.

Wang, Y. J., Wang, J., Sun, H. Q., Martinez, M., Sun, Y. X., Macia, E., Kirchhausen, T., Albanesi, J. P., Roth, M. G., and Yin, H. L. (2003). Phosphatidylinositol 4 phosphate regulates targeting of clathrin adaptor AP-1 complexes to the Golgi. Cell *114*, 299–310.